Earth Systems and Environment (2019) 3:367–379
https://doi.org/10.1007/s41748-019-00116-x

ORIGINAL ARTICLE

Effect of 1-km Subgrid Land-Surface Heterogeneity on the Multi-year Simulation of RCM-Modelled Surface Climate Over the Region of Complex Topography

Imran Nadeem[1] · **Herbert Formayer**[1] · **Asma Yaqub**[1]

Received: 8 May 2019 / Accepted: 22 August 2019 / Published online: 31 August 2019

Abstract
Effects of parameterization of subgrid-scale topography and land cover scheme (SubBATS) at 1-km resolution were investigated over the Alpine region using a regional climate model. Two multi-year simulations were carried out with the Regional Climate Model of International Centre for Theoretical Physics. The control simulation was carried out at 10-km horizontal resolution using standard land-surface model; while for the SubBATS simulation, the land-surface model was employed at much higher resolution (1 km) to investigate the effect of land-surface heterogeneity on the Alpine climate. In SubBATS, near-surface atmospheric state variables from coarse (10-km) atmospheric model were disaggregated to 1 km before passing to high-resolution land surface scheme. Comparison of these two multi-year simulation was done for the Great Alpine Region. The analysis shows the added value imparted by very high-resolution SubBATS in simulating hydrology processes in the complex terrain. The direct effects of the scheme are evident on height-dependent variables; temperature and snow pack. The better representation of topographic height in sub-scale scheme leads to more refined temperature field which subsequently results in more realistic representation of snow cover and snow melt. At 1-km resolution, the influence of resolved mountain peaks and valleys results in decrease of snow-covered area. The subgrid scheme not only improves the overall simulation by feedback process but also provides high-resolution meteorological fields that can be used for adaptation and impact studies. Therefore, more accurate representation of land-surface heterogeneity in sub-grid approach improves the temperature and snow fields over the complex terrain and can be useful for coupling with impact models, although further improvements are desirable.

Keywords Regional climate models · Subgrid heterogeneity · SubBATS scheme · Subgrid-scale topography and landuse

1 Introduction

Recent advances in computer resources, availability of high spatial resolution observations and the demand of climate information at local scale by climate-impact modellers have motivated the regional climate modelling community to apply climate modelling at increasingly higher spatial resolution using regional or global climate models. In recent years, numerous studies have proved the added value of high resolution, and hence emphasised the use of very high-resolution and even convection-permitting regional climate simulations (e.g., Termonia et al. 2018; Prein et al. 2015; Cholette et al. 2015; Ban et al. 2014; Kendon et al. 2014; Jacob et al. 2014; Chan et al. 2013; Pavlik et al. 2012; Hohenegger et al. 2008). Though the convection-permitting models (CMPs) can be deployed at horizontal resolution of less than a kilometre (e.g., Mölg and Kaser 2011; Schicker and Seibert 2009), yet the typical horizontal grid spacing used in recent high-resolution climate studies ranges from 10 to 15 km. For example, the first high-resolution climate change projections for impact studies in Europe (EURO-CORDEX) were completed with a horizontal resolution of 12.5 km (Jacob et al. 2014). Such high resolution is achieved through cascade method using multiple-grid nesting between the RCM and the driving fields. In another study, de Vries et al. (2014) performed simulations with horizontal grid spacing of 12 km to study changes of mean snowfall and

✉ Imran Nadeem
imran.nadeem@boku.ac.at

[1] Institute of Meteorology and Climatology, University of Natural Resources and Life Sciences Vienna (BOKU), Vienna, Austria

seasonal extremes. The CPMs (with horizontal grid spacing less than 4 km) which are mainly used in short-range weather forecasting are slowly propagating to regional climate modelling. Prein et al. (2015) provided an overview of all the CPM climate simulations performed to-date and considered the CPMs as a very promising tool for future climate research. For example, Kendon et al. (2012) found that precipitation over a region of the United Kingdom simulated by the 1.5-km CMP simulation is much more realistic than in the high-resolution 12-km RCM simulation. Similarly, Rasmussen et al. (2011) reported improvement in distribution of snowfall with 2-km CPM simulation compared to 36-km grid-mesh simulation. Although the convection-permitting climate simulations reduce errors in large-scale model, yet due to very high computational cost, their use in climate studies is still limited.

The regional climate models with horizontal resolution of 10 km are not capable of resolving big mountain valleys (e.g., Inn valley in Austria) in a proper way due to orographic smoothing in the model. The near-surface meteorological parameters simulated by an RCM in mountainous regions represent the situation at an average elevation within the grid box. However, accumulation and melting of snow, runoff and evaporation particularly depend on surface temperature and hence on surface topography. Even dependence of snow accumulation on changes in temperature is influenced by the surface elevation (Hantel et al. 2000). As snow cover has profound impact on surface energy budget, a realistic snow modelling is crucial for mountainous regions. For example, Rasmussen et al. (2011) found that horizontal resolution less than 6 km is required for reasonable snow accumulation in the Colorado Rocky mountains. A similar study by Garvert et al. (2007) suggested the use of grid sizes below 4 km to properly simulate snowfall over the complex terrains of Cascade mountain range in Oregon. A simulation with horizontal resolution of 4 km with a CPM would require an intensive use of computational resources; therefore, running an RCM at such a high resolution for months or multiple years is not feasible for many institutions. Therefore, we deployed an intermediate approach where benefits of high resolution were achieved using subgrid parameterization and hence reducing the dependence of climate models on spatial resolution. For example, Leung and Ghan (1995) used a mosaic scheme with different elevation classes within a grid cell to simulate the effects of sub-grid scale topographic variation when it was poorly resolved by the regional climate model. Later, a parametrization of sub-grid-scale elevation and land cover was developed and implemented in the framework of regional climate model RegCM3 (Giorgi et al. 2003). In this scheme, each coarse grid box is divided into regular, fine-scale sub-grids for calculations by the land surface model to capture the effects of subgrid scale variations arising from refined topography and land cover.

The subgrid surface scheme in RegCM3 not only produces fine-scale information at the surface but also improves overall simulation of near-surface air temperature in mountainous region, and a more realistic simulation of snow as driven by complex terrain features in the mountains (e.g., Dimri 2009; Im et al. 2010). Dimri (2009) studied the effects of subgrid scheme on surface climate over the Himalayas, where heterogeneities in topography and landuse are very high. He reported that the subgrid scheme in RegCM3 provides more realistic representation of resolvable fine-scale surface and atmospheric circulations which results in explaining mean variability in a better way. The subgrid surface scheme remarkably affects the variability of near-surface temperature and snow accumulation, as well as the winter precipitation over the Himalayan region. In most cases, the results from subgrid scheme are in better agreement with observations. Moreover, representation of the subgrid scale scheme has significant impact on the variability of the surface processes. Similarly, Im et al. (2010) evaluated results of the subgrid scheme over the European Alps. They concluded that the hydrological cycle including precipitation is not very much affected by the subgrid scheme but runoff at small-scale catchments is improved by the subgrid disaggregation.

In this paper, we have quantified the effect of SubBATS scheme at 1-km horizontal resolution on the simulated snow accumulation and snow melt and the resulting changes on the surface radiation and water budget. The present study was conducted during the EC FP6 Project CECILIA (Central and Eastern Europe Climate Change Impact and Vulnerability Assessment; Halenka 2010). In CECILIA, high-resolution (10-km) simulations over different domains of the European region were performed with RegCM3.

The paper is organised in different sections. Section 2 highlights the model, input data, observational data, evaluation methods and experiment design; whereas, the results and discussion are presented in Sect. 3. And finally, the summary and conclusions are presented in Sect. 4.

2 Model, Data and Evaluation Methods

2.1 Model

The model used in the present study is Regional Climate Model (RegCM3) which is developed and maintained by the Abdus Salam International Centre for Theoretical Physics (ICTP). RegCM3 is described in detail by Pal et al. (2007). It is a hydrostatic, limited area, primitive equation model which uses sigma-pressure as vertical coordinate. A summary of various parameterizations and physical schemes used in this study is provided as follows. The medium-resolution planetary boundary scheme developed by Holtslag et al. (1990)

and radiative transfer package of the NCAR Community Climate Model, version 3 (CCM3; Kiehl et al. 1996) were used. Fluxes from water surfaces were calculated by the scheme of Zeng et al. (1998). Large-scale precipitation processes were handled with subgrid explicit moisture scheme (SUBEX) of Pal et al. (2000). The SUBEX is a physically based parameterization scheme which calculates the auto-conversion of cloud water to rainwater, evaporation, accretion and cloud fraction at grid point level. The mass flux scheme of Grell (1993) with Fritsch and Chappel (1980) closure assumption was employed for parameterization of convective precipitation. Biosphere–atmosphere transfer scheme (BATS) version 1e (Dickinson et al. 1993) accounted for the exchanges of energy, momentum and moisture between the atmosphere and land surface. RegCM3 has already been updated to version 4 as discussed in details by Giorgi et al. (2012), but for the present study, we intentionally selected version 3 to be consistent with other studies conducted for the project. In latest version of the model, some parameters of SUBEX scheme were changed but there has been no improvement in SubBATS scheme. As discussed in Nadeem and Formayer (2015), the original version of SUBEX scheme is more suitable for our study area, which is an important factor favouring our selection of RegCM3 for this study.

2.2 Subgrid Parameterization

The biosphere–atmosphere transfer scheme (BATS) is the standard land surface model in RegCM3. BATS is responsible for the exchange of energy, water, and momentum between the surface and atmosphere through the atmospheric boundary layer (Dickinson et al. 1993). The SubBATS scheme adopts a regular fine-scale surface subgrid for each coarse grid cell of model domain. Meteorological variables are disaggregated from the coarse model grid to the fine grid based on the elevation difference between the subgrid and corresponding coarse grid cells. With this disaggregation procedure, low-elevation subgrid cells are characterised by higher 2-m temperature and water vapour mixing ratio than high-elevation subgrid cells. During the simulation, land-surface calculations are performed separately for each subgrid cell and then surface fluxes are re-aggregated onto the coarse grid cell for input to the atmospheric model. Precipitation does not correlate easily either with elevation or with land cover type; therefore, precipitation disaggregation is not straightforward. Only subgrid disaggregation of temperature and water vapour has been implemented (Giorgi et al. 2003). The large-scale precipitation flux at each subgrid cell is the same as for the corresponding coarse grid cell. However, the convective precipitation is randomly distributed over 30% of the subgrid cells. Despite the limitations, the subgrid surface scheme is a cheap and effective alternative to convection-permitting simulations.

2.3 Input Data

As a lateral boundary condition (LBC), we used the gridded reanalysis data, ERA-Interim with resolution of $0.7° \times 0.7°$ (Dee et al. 2011) provided by European Centre for Medium-Range Weather Forecasts (ECMWF). The weekly optimum interpolation (OI) sea surface temperature (SST) analysis version 2 was used as surface boundary conditions (Reynolds et al. 2002). The OISST, produced by NOAA, has resolution of 1°. In RegCM3, LBCs and SST are updated every 6-hourly through the relaxation method explained by Giorgi et al. (1993). The high-resolution ERA-Interim used in this study is available to registered users through C3S Climate Data Store (CDS) implemented by ECMWF. High-resolution SubBATS at 1 km also require accurate digital elevation model (DEM) data with horizontal resolution of less than 1 km. Similarly, sub-kilometre scale land cover information is also necessary for the simulations. Such a high-resolution input DEM and Land cover are not supported by the default version of the RegCM3 and hence, input terrain code was modified to implement these high-resolution input datasets. We used near-global DEM from Shuttle Radar Topography Mission (SRTM) and land cover from Global Coverage and Global Land Cover Characterization (GLCC) at resolution of 30 arc-sec (~ 900 m). Both SRTM30 and GLCC30 are freely available from the official website of United States Geological Survey (USGS).

2.4 Experiment Design

To find the best setup for multi-year SubBATS simulation, we performed a suite of 1-year-long hindcast simulations with different lateral boundary conditions, domain size and nesting techniques. The results of our sensitivity studies suggested the use of direct nesting with high-resolution ERA-interim and not too big domain size (Nadeem and Formayer 2015). Control and SubBATS simulations were performed for 6-year period from Jan 1999 to Dec 2004. The model was, however, initialized on October 1, 1998 to allow 3 months of spin-up time. The topography and land cover for the control simulation at 10-km resolution and the SubBATS simulation at 1 km are shown in Figs. 1 and 2, respectively. The Great Alpine Region defined in the Alpine Convention (Chatré et al. 2010) is highlighted with thick white line. The more realistic representation of Alpine valleys and mountain ridges in the SubBATS experiment can be clearly seen. In Fig. 3, frequency distribution of elevation is shown for both experimental setups for the Alpine region. The control experiment underestimate very low and very high altitudes, due to smoothing at the coarser resolution.

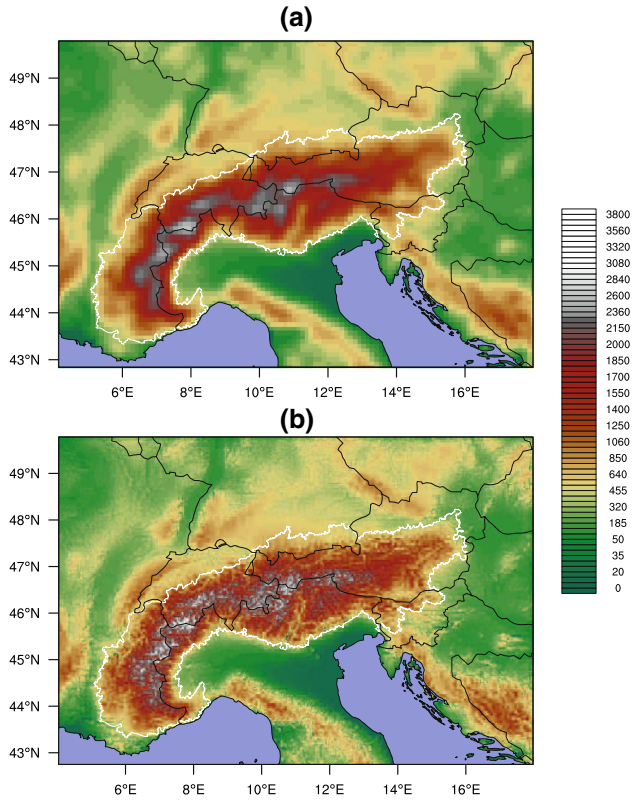

Fig. 1 RegCM3 domain showing topography at 10-km (BATS) and 1-km (SubBATS) resolutions

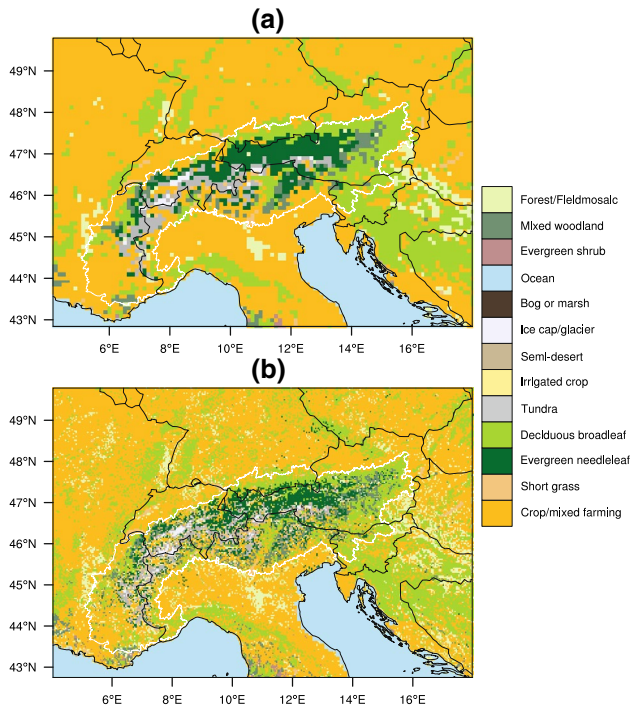

Fig. 2 Landuse types of 10-km BATS and 1-km SubBATS domains

2.5 Reference Data

Observed gridded precipitation data obtained from Swiss Federal Institute of Technology, Zurich ETHZ were used for evaluation of precipitation (Isotta et al. 2014). The daily observed gridded precipitation (hereafter EURO4M) covers the European Alps and surrounding flat areas (4.8–17.5° E/43–49°N). The distribution of precipitation is estimated for all days of the period 1971–2008. Estimates are based on data from more than 8500 weather stations of meteorological and hydrological services. The analysis is provided on a regular grid in the ETRS89-LAEA projection, with a grid size of 5 × 5 km. The high density of observational input data contributes to quantitative accuracy and high effective resolution (approx. 10–20 km) of precipitation estimates in the source region of four major European rivers. A detailed description of and climatological analysis with this dataset are given by Isotta et al. (2014). The EURO4M precipitation data were upscaled to RegCM3 grid using grid remapping routines of Earth System Modelling Framework (ESMF) developed by NOAA, USA. To ensure that area average do not change after regridding from one grid to another, the conservative remapping method was used (Jones 1999). For evaluation of temperature, we used high-resolution European daily gridded temperature dataset produced using the European Climate Assessment and Dataset (ECA&D) blended daily station data. These observed temperature data (hereafter E-OBS; Haylock et al. 2008) are available 0.25° regular lat-lon grid and covers Europe and parts of Middle East and Northern Africa. For current study, version 14.0 of E-OBS was used. The RegCM3 simulated temperature was re-sampled to E-OBS grid and also corrected according to elevation differences.

2.6 Evaluation Methods

The evaluation of daily modelled temperature and precipitation was carried out using skill-scores discussed in detail by Nadeem and Formayer (2015). The total skill score is weighted sum of bias skill score and Fischer's skill score. The bias skill score accounts for model's ability to reproduce absolute values of a variable whereas the Fischer's skill score is measure of the accuracy of a model to produce correct spatial distribution of a meteorological field in consideration. The value of total skill score of a field lies between 0 and 1.0, where 1.0 indicates a perfect agreement of the model with observations. The total skill score which is basically the measure of model's spatial performance was calculated on daily basis.

To compare simulated snow with observed snow in the Austrian Alps, both quantities have to be in the same unit. The observed snow measurements at stations, by the Central Institute for Meteorology and Geodynamics, Austria

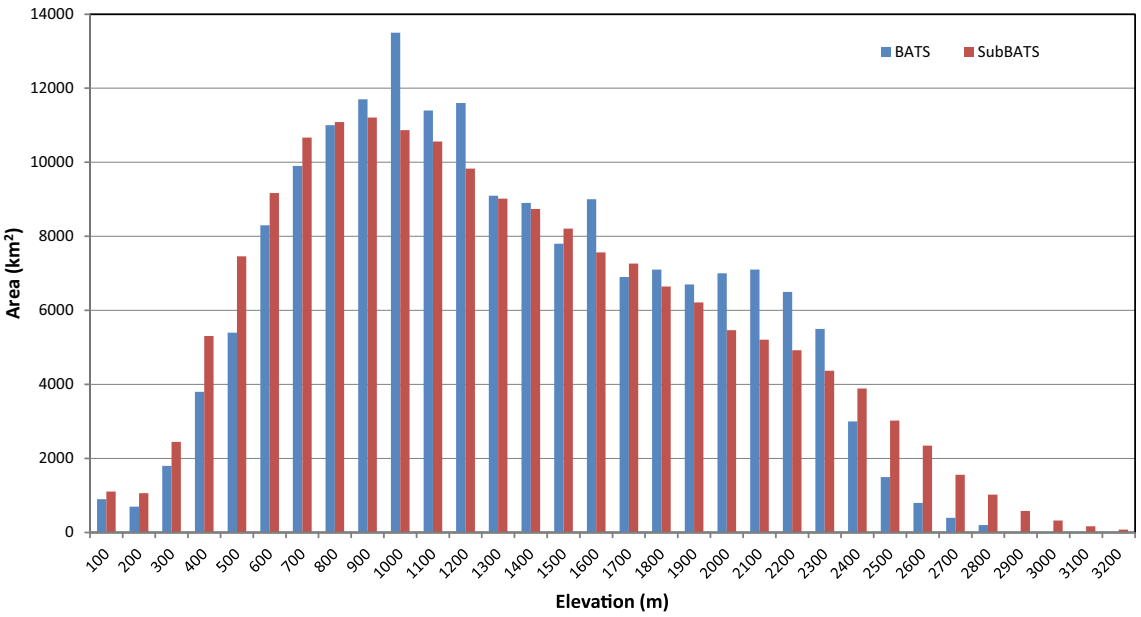

Fig. 3 Histogram of elevation distribution of the Alpine region for BATS and SubBATS

(ZAMG) are recorded as snow depth in metre. However, the model output gives snow water equivalent (SWE) in units of mm. As SWE has more hydrological significance, we converted observed snow density to snow water equivalent for comparison. Jonas et al. (2009) developed a regression model based on 11,147 records of snow densities and depths measured in Swiss Alps, to calculate SWE from four factors. In order of relevance, these factors are: season, snow depth, station elevation, and climate region. The snow depth (HS), bulk density (ρb), and snow water equivalent (SWE) are interconnected to one another through this relation:

$$\mathrm{SWE}_{\mathrm{mod}} = \mathrm{HS}_{\mathrm{obs}} \times \rho b_{\mathrm{mod}}, \quad (1)$$

where ρb is given by:

$$\rho b_{\mathrm{mod}} = a \times \mathrm{HS}_{\mathrm{obs}} + b + \mathrm{offset}_{\mathrm{reg}} \quad (2)$$

In both Eqs. (1) and (2), SWE is given in kg/m^2, HS has units m, and ρb is expressed in kg/m^3. The values of pair (b, a) are given in Table 1. The least significant quantity offset$_{\mathrm{reg}}$ has no value for the Austrian Alps; therefore, we set it to zero for our calculations.

Table 1 Regression coefficients (b, a) to calculate snow water equivalent (SWE) from snow density according to Eqs. (4) and (5) (source: Jonas et al. (2009))

Altitude	≥ 2000 m	≥ 1400 m and < 2000 m	≤ 1400 m
October	na.	na.	na.
November	(206, 47)	(183, 35)	(149, 37)
December	(203, 52)	(190, 47)	(201, 26)
January	(206, 52)	(208, 47)	(235, 31)
February	(217, 46)	(218, 52)	(279, 9)
March	(272, 26)	(281, 31)	(333, 3)
April	(331, 9)	(354, 15)	(347, 25)
May	(378, 21)	(409, 29)	(413, 19)
June	(452, 8)	na.	na.
July	(470, 15)	na.	na.

The na. values mean too little data is available to establish a regression model

3 Results and Conclusions

3.1 Control Simulation Versus Observations

In this section, we compared the model simulated precipitation and 2-m temperature against observation. Instead of showing spatial plots of absolute values or bias plots calculated against observations, we employ a more sophisticated approach by comparing model against observation using skill-scores. The total skill-scores (TSS) which are weighted sum of Fischer's Skill Scores (FSS) and Bias Skill Scores (BSS) represent the spatial correlation and biases between the model and observations. The TSS also show the model agreement with observation on temporal scale. The TSS are calculated on daily basis for simulated precipitation versus EURO4M and for modelled 2-m temperature versus E-OBS. Monthly means of the daily scores for each year along with monthly climatologies for the 6-year period are plotted and shown in Fig. 4. For precipitation equal weightage is given to both scores; TSS $= \alpha$ FSS $+ (1 - \alpha)$ BSS, where $\alpha = 0.5$.

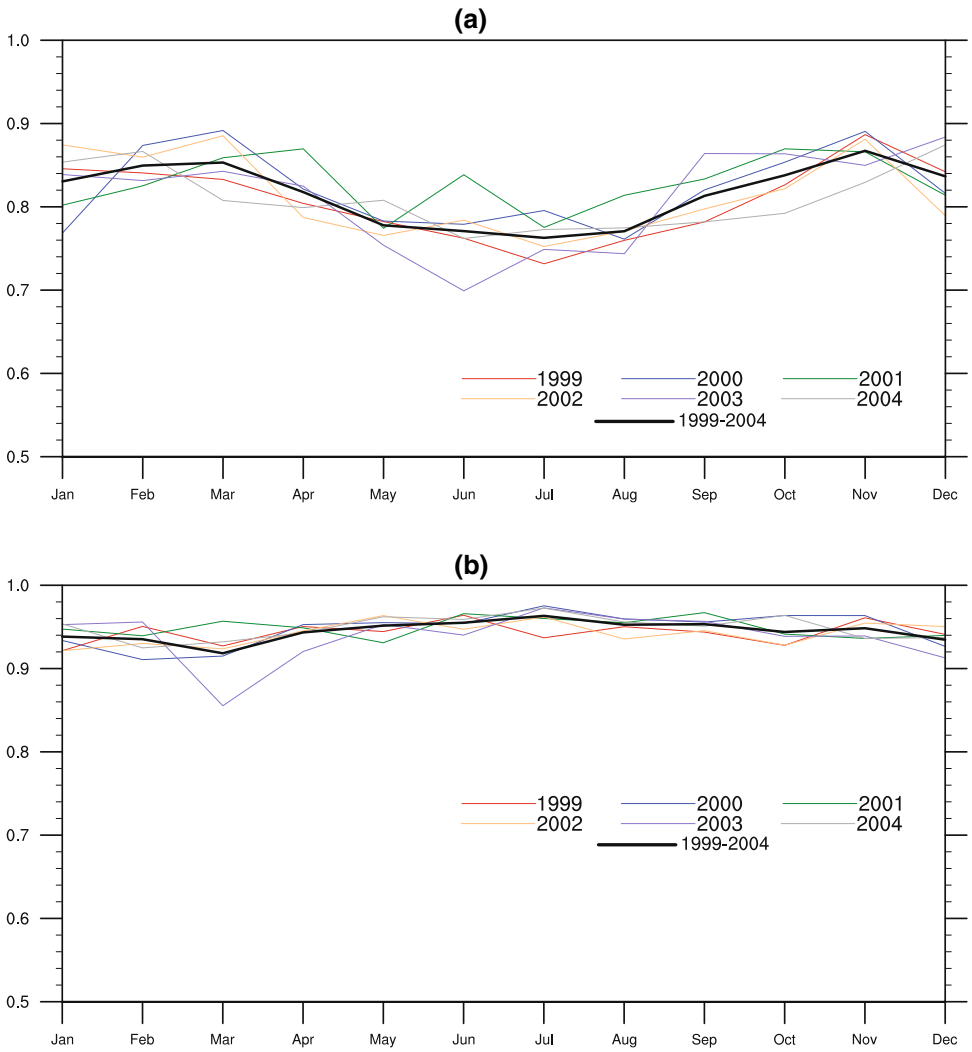

Fig. 4 Monthly total skill-scores calculated for each year for **a** precipitation and **b** 2-m temperature

As temperature is mostly well correlated within the Alpine region, more weightage is given to BSS by choosing $\alpha = 0.4$. The upper panel shows the TSS for precipitation for each year of the simulation. The model shows higher skill in simulating precipitation in winter months than in summer. This is because RegCM3, like other models, is not very efficient in simulating Mediterranean cyclones and small-scale convective events which are responsible for most of the precipitation in the Alpine region in summer.

In general, the model shows good agreement with observations. The lower panel shows TSS for 2-m temperature. It is evident that the model performs equally well in all months and no annual cycle can be seen in the TSS. The higher skill scores for temperature can be explained by the more homogeneous structure of temperature field compared to the precipitation field. The skill scores are dominated by correct representation of the dynamics within the model (e.g., pressure distribution, baroclinicity). As the dynamical part for the BATS and SubBATS versions of the model is the same, skill score does not differ significantly between the two different setups. In general, the results of skill score analysis indicate an appropriate set up of the model.

3.2 BATS Versus SubBATS

As the disaggregation in SubBATS scheme is mainly based on elevation, its direct affects are evident on height-dependent variables; temperature and snow pack. In Fig. 5a, d, near-surface air temperature for BATS and SubBATS is shown. The better representation of topographic height in sub-scale scheme leads to more realistic temperature field which subsequently enhances snow accumulation in the Alps. In Fig. 5b, e average snow accumulation and in Fig. 5c, f average of the number of days with snow cover (snow water equivalent > 2 mm) are shown for the period 1999–2004. At 1-km resolution, influence of resolved mountain peaks and valleys results in decrease of snow-covered area. This can also be seen in domain average values on the upper right corner of each plot. In the sub-scale simulation, there is 10% reduction in fraction of snow-covered

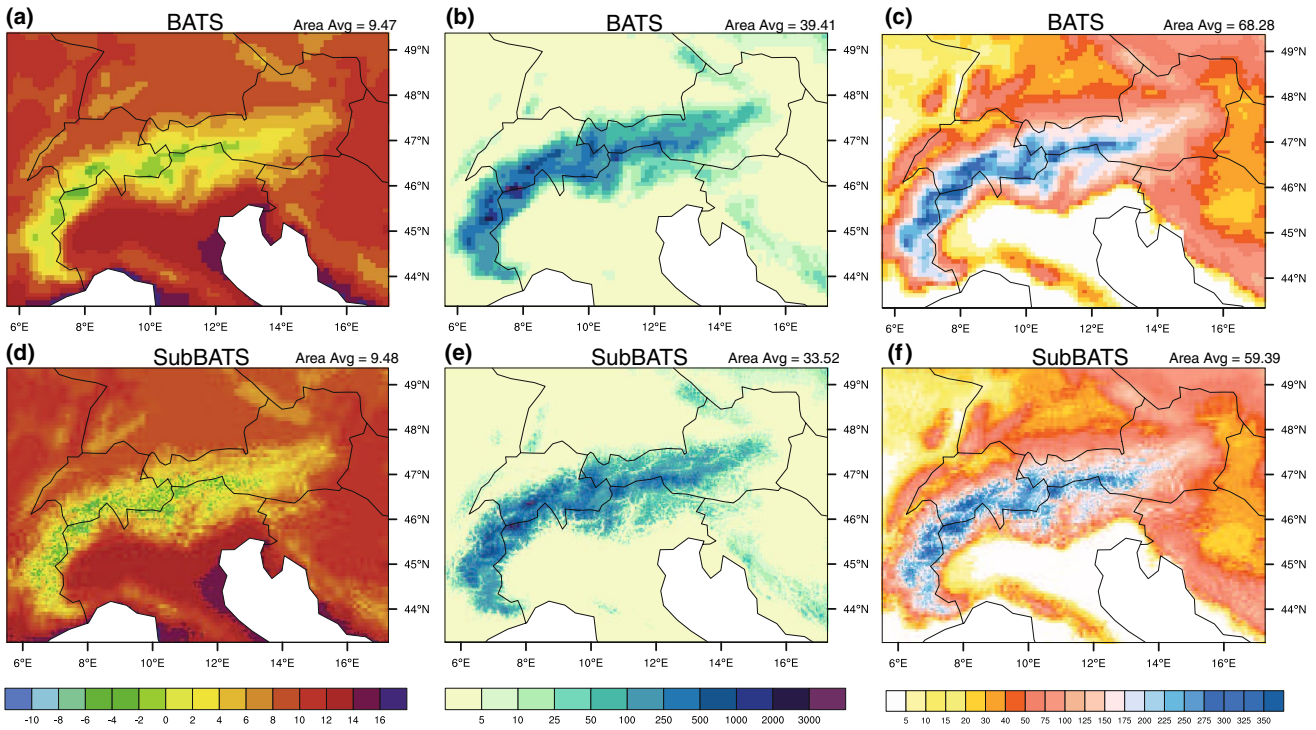

Fig. 5 Annual 2-m temperature distribution for BATS (**a**) and SubBATS (**d**) in Celsius, annual snow distribution for BATS (**b**) and SubBATS (**e**) in water equivalent (mm) and annual snow-covered days for BATS (**c**) and SubBATS (**f**) for 1999–2004

area (Fig. 5e). Comparison of large-scale and connvective precipitation between the two simulations is presented in Fig. 6. As expected, there is almost no difference in large-scale precipitation between BATS and SubBATS. However, connvective precipitation is slightly modified because of changed snow-cover area leading to changes in incoming and absorbed solar radiations. The averaged fraction of snow-covered area per day is given in Fig. 7. The reduced fraction of snow-covered area during winter and spring within SubBATS stems from a more realistic representation of the Alpine valleys with areas below 1000 AMSL, which are frequently not snow covered even in winter. The difference increases during spring, indicating a more realistic snow melt in the SubBATS run. During summer, the difference is negligible and in autumns, SubBATS has even a higher fraction of snow cover due to a better representation of mountain ridges with elevations higher than 2500 AMSL. The effect is better understood with histogram plots of monthly snow cover (mm H_2O) for different elevations bands (see Fig. 8). The first histogram on the top left represents all elevation in the alpine region (shown with white border line in Fig 1) and the rest of histograms represent areas above 500-, 1000-, 1500-, 2000- and 2500-m AMSL. The areas covered by BATS and SubBATS model for different elevation ranges are given on the top of each plots in units of × 100 km^2. For the whole Alps and for all grid boxes above 500 m, the BATS simulation has more snow cover area, which can be explained with the help of a histogram of elevation distribution of BATS and SubBATS presented in Fig. 3. At lower elevations, valleys that are properly resolved only by SubBATS are not covered with snow throughout the year, leading to lower snow cover shown by SubBATS in the first two histograms. The effect changes as grid boxes with elevations above 1000 m are considered. Above 1000 m, during the accumulation months November to March or even April (for very high elevations), SubBATS has more snow owing to high peaks only seen by 1-km resolution. This effect reverses in melting months because of the fast melting of snow at lower elevations in SubBATS. The huge overestimation of the area between elevations 900 and 1300 m in Fig. 3 explains this effect. A 10 km grid with an average elevation of 1000 m may include valleys with elevations of 500 m and mountains peaks of 1500 m. The flattening of mountain peaks leads to less snow in the accumulation period in BATS and misrepresentation of valleys resulting in more snow in BATS in ablation months. Above 2500 m, SubBATS retains more snow for all months. This is because of very high peaks, which are only seen by SubBATS model, are covered with snow throughout the year.

These effects of subgrid scheme on surface energy fluxes are also studied. However, in the Alps, the effect of SubBATS on energy fluxes is quite complex. The locally different surface temperature distributions affect the convection resulting in modified cloudiness and even altered

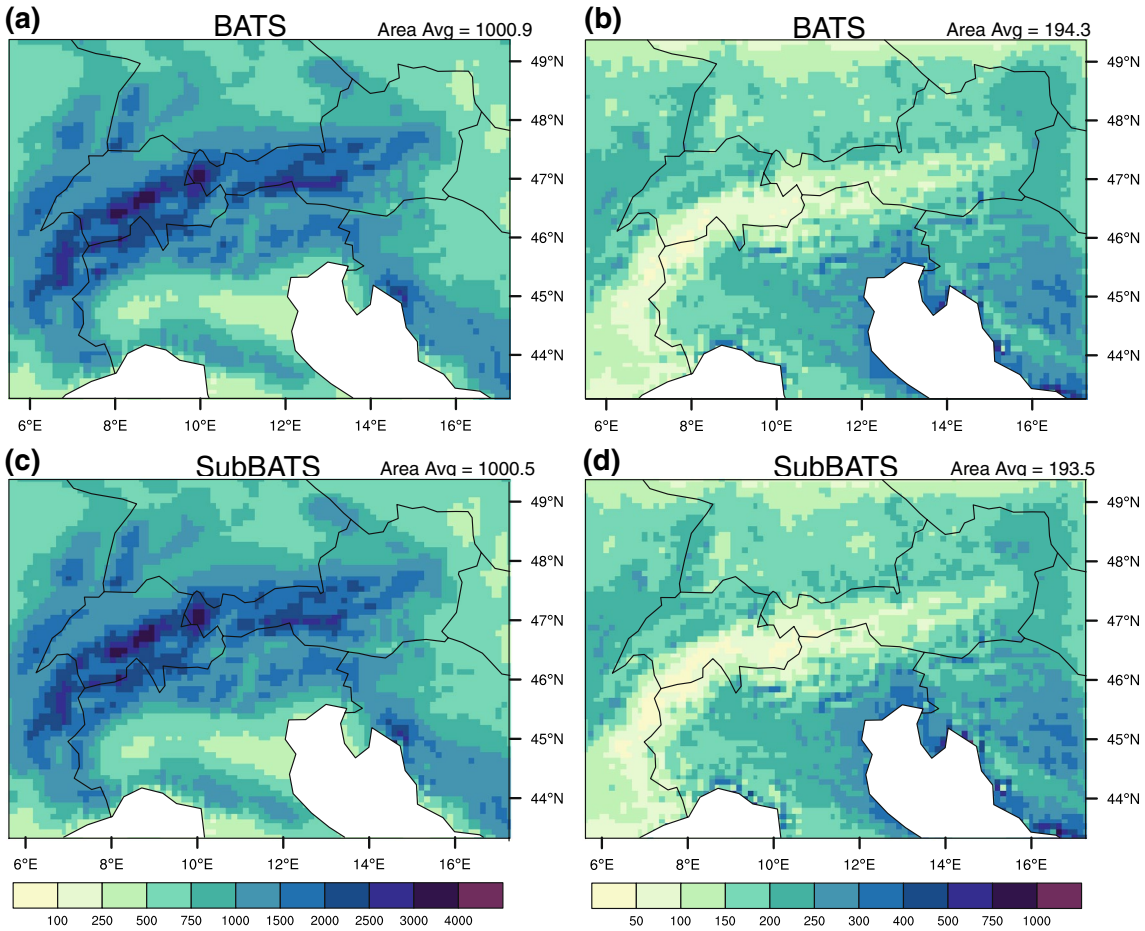

Fig. 6 Mean annual large-scale precipitation for BATS (**a**) and SubBATS (**c**) in mm/year and mean annual connvective precipitation for BATS (**b**) and SubBATS (**d**) for the period 1999–2004

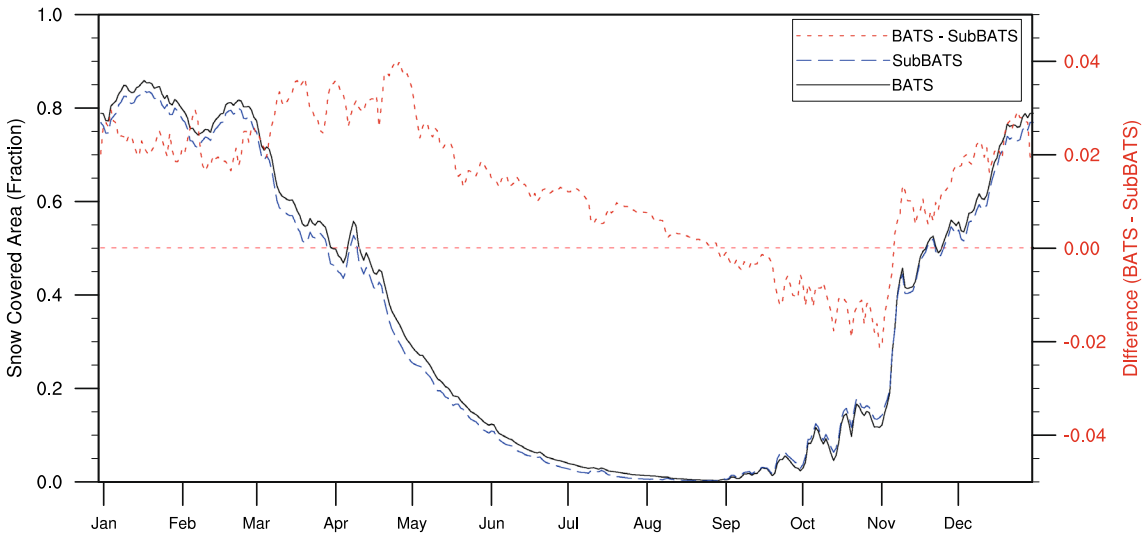

Fig. 7 Daily climatology of fraction of snow-covered area of Alpine region for the period 1999–2004. The right *Y*-axis represents the difference line plotted by a red dotted Line

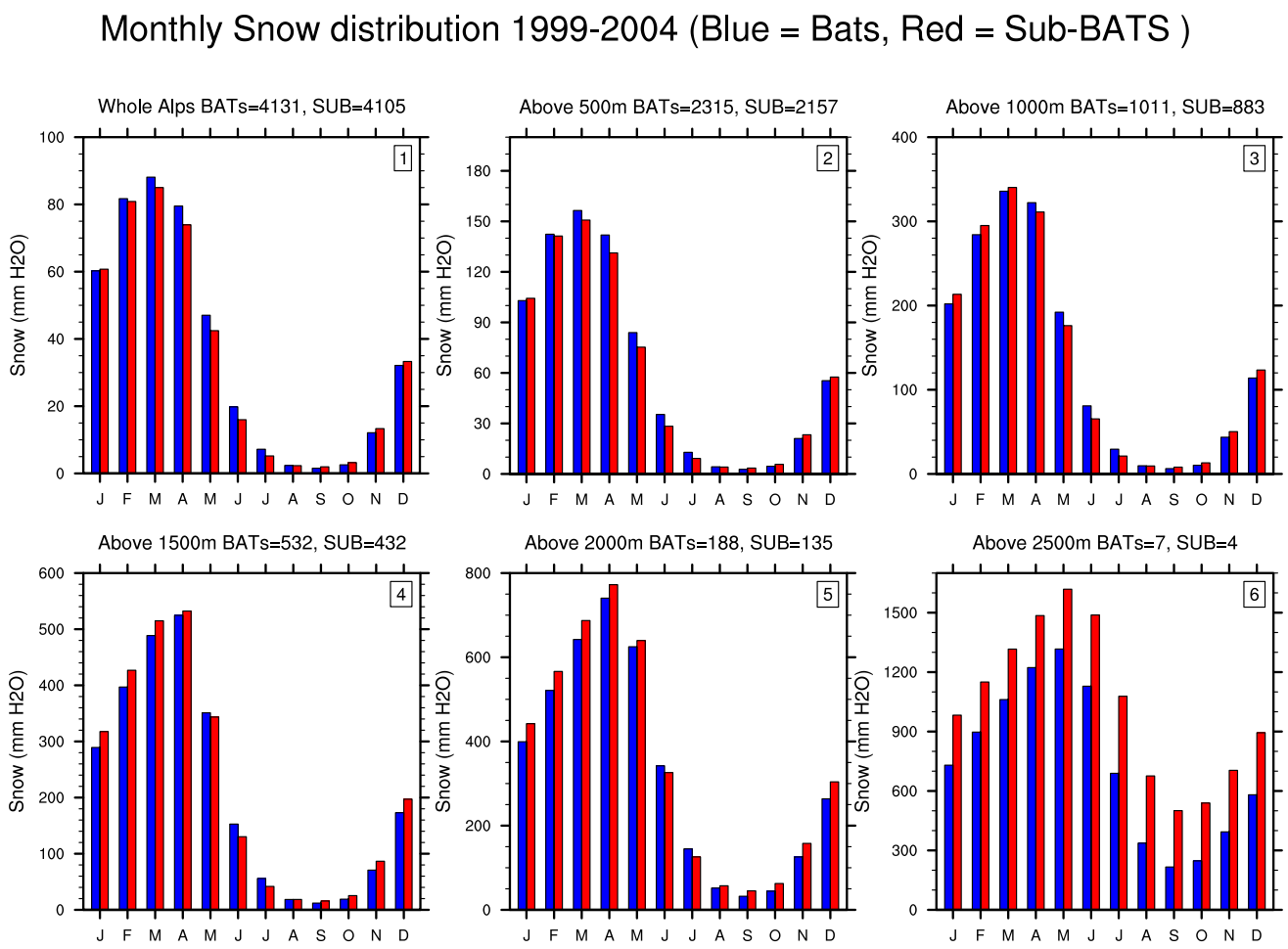

Fig. 8 Monthly snow distribution for whole Alps and for different elevation bands in SWE (mm H_2O) 1999–2004

precipitation. There is no combined effect on the total precipitation but a change in the convective precipitation in summer, as the differences between the BATS and SubBATS simulations are highest in May and August, and negligible during fall and winter.

3.3 Catchment Analysis

The subgrid scheme not only improves the overall simulation by feedback process but also provides high-resolution meteorological fields that can be used for adaptation and impact studies. In the above section, we have analysed the whole alpine domain. In this section, we present the analysis of a selected catchment in the Salzach region in Austria. The catchment along with the Salzach river is shown in Fig. 9. The analysis of snow-covered area of the whole catchment represented by BATS and SubBATS is no different than the results for whole Alps shown in Fig. 7; therefore, we focus on comparison of SubBATS modelled snow (at 1-km grid) with observed snow depth measurements from ZAMG. For this comparison, we select a mountain station and a valley

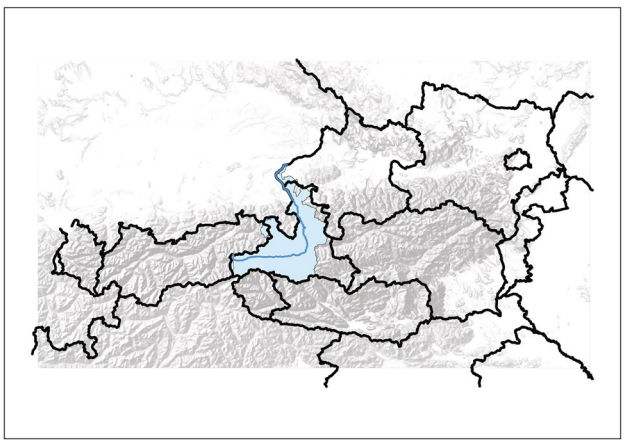

Fig. 9 Salzach catchments for detailed analysis. The blue area represents the catchment and blue line shows the Salzach river

station: Schmittenhöhe (1950 m) and Zell-am-See (770 m). Both stations are located in the Salzach region.

The observed snow depth from these two station is converted into the snow water equivalent (SWE) using the method discussed in the Sect. 2.6. The comparison of daily climatology of SWE for years 1999–2004 is presented in Fig. 10. Both stations are located in one coarse grid cell which covers an area of 100 km^2. The elevation of the BAT grid cell lies between the elevations of the two sites which explains the huge overestimation of SWE for the valley station and underestimation of SWE for the mountain station. For both locations, however, the annual cycle of snow cover is very well captured by the SubBATS simulation. The SubBATS tends to overestimate snow cover in spring at the mountain site and underestimate snow at the valley station for the same period. During the ablation period, the agreement between the model and observation is astonishing. The results indicate that the high-resolution meteorological fields outputted by SubBATS are reliable and can be used for impact studies (e.g., hydrological processes).

We further analysed solar radiations in Salzach catchment as shown in Fig. 11. The results show that there is clear annual cycle observed in the difference between absorbed solar radiation from the two simulations. The SubBATS simulation shows increase of up to 4 W/m^2 in the daily climatology of absorbed radiation calculated over the 6-year period. The difference is almost negligible in winter but it becomes significant in March when snow cover starts to melt at the lower elevations. The maximum difference observed in June corresponds to bigger differences in the snow covered

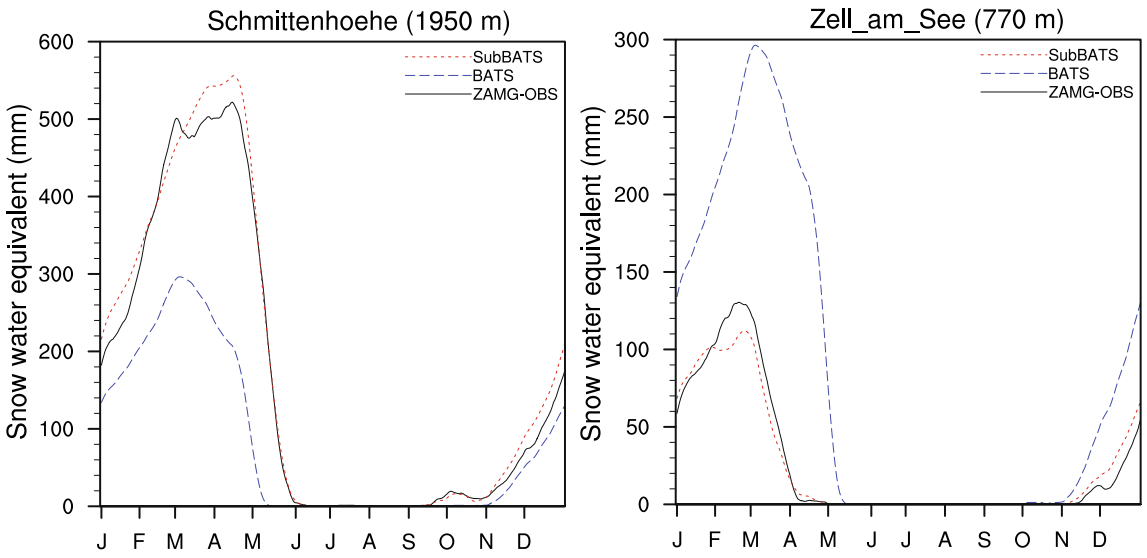

Fig. 10 Daily climatology of snow water equivalent for selected stations in Salzach catchment for the period 1999–2004

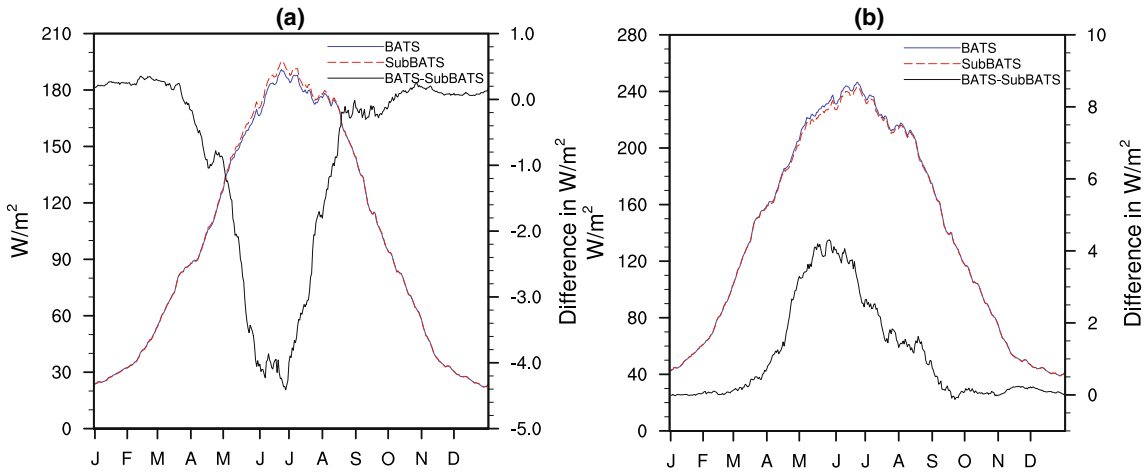

Fig. 11 Daily climatology of **a** absorbed solar radiation and **b** incoming solar radiation for Salzach catchment for the period 1999–2004

area in both simulations. This trend continues till autumn, when difference between the two runs reduces to zero by the end of August. The sharp reduction in August also suggests that the increase in absorbed radiation mainly depends on different snow cover resulting from resolved topography in SubBATS and does not stems from the heterogeneity of subgrid scale land cover. In Fig. 11b, the effect of SubBATS on incident solar radiation is also shown. There is no significant difference found in daily climatologies of incident solar radiation during the winter. However, starting from April, incident solar radiation starts to decrease in SubBATS simulation presumably triggered by the onset of thermally induced convection. The difference continues to widen till May and June when the highest difference of about 4 W/m^2 is observed followed by a sharp decrease in July and August. But this dissimilarity reduces to roughly zero by the end of September. The effect can be attributed to convective clouds induced by finer temperature structure resulting from land-surface heterogeneities in the SubBATS simulations. This depletion in incoming solar radiation in sub-scale scheme has the same timing and magnitude as the increased absorbed solar radiation in the Salzach valley because of snow-albedo feedback.

4 Summary and Conclusion

The paper presents the analysis of 6-year simulations with the regional climate model RegCM3 using two different landuse schemes, BATS and SubBATS, within the Alpine region with a spatial resolution of the surface model of 10 km and 1 km, respectively. Both models show good performance concerning daily precipitation and temperature on the 10-km scale. Within the complex topography of the Alpine region, the 10-km BATS run clearly shows limitation in the representation of the real topography, leading to an underestimation of low elevations below 900 AMSL and high elevations beyond 2500 AMSL. This results mainly in a smoothed temperature field, underestimating the temperatures in the valleys and overestimating at the ridges as can be seen in Fig. 5a, d. On the other hand, the higher spatial resolution of SubBATS not only affects the instantaneous fields like temperature or humidity, but also improves the accumulative variables like snow. The snow accumulation and melt processes within the Alpine valleys are much better represented by SubBATS simulation as in BATS (Fig.7). As snow highly impacts the surface energy budget, a realistic snow cover is important to simulate an accurate micro climate, including soil water content and soil temperature. In comparison to the previous studies done with SubBATS (e.g., Dimri 2009; Im et al. 2010), we have used the highest resolution (1 km) used so far in SubBATS studies. Our results are not only consistent with previous studies but also provide more insight into annual snow accumulation and melt cycle. For example, in 6-month-long simulation (Oct–Mar) of SubBATS at 10 km compared to 60-km BATS simulation over the Himalayan region, Dimri (2009) found greater overall snow amounts in the subgrid experiment. This is partially in-line with our results showing increase in snow-cover area in SubBATS in autumn. Actually, to proper understand the effect of SubBATS on simulation snow, 6-month simulation is too short and 10-km resolution is too coarse to resolve Himalayan region in a proper way. A better study was performed by Im et al. (2010) where a 10-year-long simulation with SubBATS at 3-km horizontal resolution and control simulation at 15-km resolution were compared for the Alpine Region. They found that the SubBATS scheme produces more refined and apparently more realistic snow patterns on account of enhanced topographic representation. They also found that on average, the snow depths are reduced in the subgrid scheme and runoff at small-scale catchments appears to be improved by the SubBATS simulation. Our study is consistent with these findings and going down to 1-km resolution has further enhanced the difference between control and SubBATS simulations. Overall, the use of the sub-scale landuse scheme SubBATS has the ability to improve the temperature field within complex terrain like the Alpine region significantly. This directly leads to a more realistic representation of snow cover and -melt, and thus to more realistic surface energy budget. The use of SubBATS resolving the Alpine valley might even alter and improve the climate change signal in climate scenario runs, due to a more reliable representation of the snow-albedo feedback.

Acknowledgements This study presented in this paper was partially funded by EC project CECILIA. The scholarship provided by Higher Education Commission of Pakistan to first author also helped to complete this study. We acknowledge the E-OBS dataset from the EU-FP6 project UERRA (http://www.uerra.eu) and the data providers in the ECA&D project (https://www.ecad.eu). Our special thanks to ECMWF for providing ERA-Interim reanalysis data. We are also very thankful to Swiss Federal Institute of Technology Zürich for providing observational precipitation dataset for this study.

References

Ban N, Schmidli J, Schaer C (2014) Evaluation of the convection-resolving regional climate modeling approach in decade-long simulations. J Geophys Res Atmos. https://doi.org/10.1002/2014JD021478

Chan SC, Kendon EJ, Fowler HJ, Blenkinsop S, Ferro CAT, Stephenson DB (2013) Does increasing the spatial resolution of a regional climate model improve the simulated daily precipitation? Climate Dyn 41(5):1475–1495. https://doi.org/10.1007/s00382-012-1568-9

Chatré B, Lanzinger G, Macaluso M, Mayrhofer W, Morandini M, Onida M, Polajnar B (2010) The Alps: people and pressures in the mountains, the facts at a glance. Permanent secretariat of the alpine convention, Insbruck, Austria. https://www.alpco

nv.org/fileadmin/user_upload/publikationen/vademecum/Vademecum_web.pdf
Cholette M, Laprise R, Thériault JM (2015) Perspectives for very high-resolution climate simulations with nested models: illustration of potential in simulating St. Lawrence River Valley channelling winds with the fifth-generation canadian regional climate model. Climate 3(2):283. https://doi.org/10.3390/cli3020283. http://www.mdpi.com/2225-1154/3/2/283
de Vries H, Lenderink G, van Meijgaard E (2014) Future snowfall in western and central Europe projected with a high-resolution regional climate model ensemble. Geophys Res Lett 41(12):4294–4299. https://doi.org/10.1002/2014GL059724
Dee DP, Uppala SM, Simmons AJ, Berrisford P, Poli P, Kobayashi S, Andrae U, Balmaseda MA, Balsamo G, Bauer P, Bechtold P, Beljaars ACM, van de Berg L, Bidlot J, Bormann N, Delsol C, Dragani R, Fuentes M, Geer AJ, Haimberger L, Healy SB, Hersbach H, Hólm EV, Isaksen L, Kållberg P, Köhler M, Matricardi M, McNally AP, Monge-Sanz BM, Morcrette JJ, Park BK, Peubey C, de Rosnay P, Tavolato C, Thépaut JN, Vitart F (2011) The ERA-Interim reanalysis: configuration and performance of the data assimilation system. Q J R Meteorol Soc 137(656):553–597. https://doi.org/10.1002/qj.828
Dickinson RE, Henderson-Sellers A, Kennedy PJ (1993) Biosphere-atmosphere transfer scheme (BATS) Version 1e as coupled to the NCAR community climate model. NCAR Technical Note NCAR/TN-387+STR. https://doi.org/10.5065/D67W6959
Dimri A (2009) Impact of subgrid scale scheme on topography and landuse for better regional scale simulation of meteorological variables over the western Himalayas. Climate Dyn 32:565–574. https://doi.org/10.1007/s00382-008-0453-z
Fritsch J, Chappel C (1980) Numerical prediction of convectively driven mesoscale pressure systems. Part I: convective parameterization. J Atmos Sci 37(8):1722–1733. https://doi.org/10.1175/1520-0469(1980)037<1722:NPOCDM>2.0.CO;2
Garvert MF, Smull B, Mass C (2007) Multiscale mountain waves influencing a major orographic precipitation event. J Atmos Sci 64(3):711–737. https://doi.org/10.1175/JAS3876.1
Giorgi F, Marinucci M, Bates G, Decanio G (1993) Development of a second-generation regional climate model (RegCM2). Part II: convective processes and assimilation of lateral boundary conditions. Mon Weather Rev 121(10):2814–2832. https://doi.org/10.1175/1520-0493(1993)121<2814:DOASGR>2.0.CO;2
Giorgi F, Francisco R, Pal J (2003) Effects of a subgrid-scale topography and land use scheme on the simulation of surface climate and hydrology. Part I: effects of temperature and water vapor disaggregation. J Hydrometeorol 4(2):317–333. https://doi.org/10.1175/1525-7541(2003)4<317:EOASTA>2.0.CO;2
Giorgi F, Coppola E, Solmon F, Mariotti L, Sylla MB, Bi X, Elguindi N, Diro GT, Nair V, Giuliani G, Turuncoglu UU, Cozzini S, Guettler I, O'Brien TA, Tawfik AB, Shalaby A, Zakey AS, Steiner AL, Stordal F, Sloan LC, Brankovic C (2012) RegCM4: model description and preliminary tests over multiple CORDEX domains. Climate Res 52(1,29):7–29. https://doi.org/10.3354/cr01018
Grell G (1993) Prognostic evaluation of assumptions used by cumulus parameterizations. Mon Weather Rev 121(3):764–787. https://doi.org/10.1175/1520-0493(1993)121<0764:PEOAUB>2.0.CO;2
Halenka T (2010) Cecilia-EC FP6 project on the assessment of climate change impacts in central and eastern Europe. In: Alexandrov V, Gajdusek MF, Knight CGF, Yotova A (eds) Global environmental change: challenges to science and society in Southeastern Europe. Springer, Amsterdam, pp 125–137. https://doi.org/10.1007/978-90-481-8695-2_11
Hantel M, Ehrendorfer M, Haslinger A (2000) Climate sensitivity of snow cover duration in Austria. Int J Climatol 20(6):615–640. https://doi.org/10.1002/(SICI)1097-0088(200005)20:6<615::AID-JOC489>3.0.CO;2-0
Haylock MR, Hofstra N, Tank AMGK, Klok EJ, Jones PD, New M (2008) A European daily high-resolution gridded data set of surface temperature and precipitation for 1950–2006. J Geophys Res Atmos. https://doi.org/10.1029/2008JD010201
Hohenegger C, Brockhaus P, Schaer C (2008) Towards climate simulations at cloud-resolving scales. Meteorol Z 17(4, SI):383–394. https://doi.org/10.1127/0941-2948/2008/0303
Holtslag A, Debruijn E, Pan H (1990) A high resolution air mass transformation model for short-range weather forecasting. Mon Weather Rev 118(8):1561–1575. https://doi.org/10.1175/1520-0493(1990)118<1561:AHRAMT>2.0.CO;2
Im ES, Coppola E, Giorgi F, Bi X (2010) Validation of a high-resolution regional climate model for the alpine region and effects of a subgrid-scale topography and land use representation. J Climate 23(7):1854–1873. https://doi.org/10.1175/2009JCLI3262.1
Isotta FA, Frei C, Weilguni V, Tadic MP, Lassegues P, Rudolf B, Pavan V, Cacciamani C, Antolini G, Ratto SM, Munari M, Micheletti S, Bonati V, Lussana C, Ronchi C, Panettieri E, Marigo G, Vertacnik G (2014) The climate of daily precipitation in the Alps: development and analysis of a high-resolution grid dataset from pan-Alpine rain-gauge data. Int J Climatol 34(5):1657–1675. https://doi.org/10.1002/joc.3794
Jacob D, Petersen J, Eggert B, Alias A, Christensen OB, Bouwer LM, Braun A, Colette A, Déqué M, Georgievski G, Georgopoulou E, Gobiet A, Menut L, Nikulin G, Haensler A, Hempelmann N, Jones C, Keuler K, Kovats S, Kröner N, Kotlarski S, Kriegsmann A, Martin E, van Meijgaard E, Moseley C, Pfeifer S, Preuschmann S, Radermacher C, Radtke K, Rechid D, Rounsevell M, Samuelsson P, Somot S, Soussana JF, Teichmann C, Valentini R, Vautard R, Weber B, Yiou P (2014) EURO-CORDEX: new high-resolution climate change projections for European impact research. Reg Environ Change 14(2):563–578. https://doi.org/10.1007/s10113-013-0499-2
Jonas T, Marty C, Magnusson J (2009) Estimating the snow water equivalent from snow depth measurements in the Swiss Alps. J Hydrol 378(1–2):161–167. https://doi.org/10.1016/j.jhydrol.2009.09.021
Jones P (1999) First- and second-order conservative remapping schemes for grids in spherical coordinates. Mon Weather Rev 127(9):2204–2210. https://doi.org/10.1175/1520-0493(1999)127<2204:FASOCR>2.0.CO;2
Kendon EJ, Roberts NM, Senior CA, Roberts MJ (2012) Realism of rainfall in a very high-resolution regional climate model. J Climate 25(17):5791–5806. https://doi.org/10.1175/JCLI-D-11-00562.1
Kendon EJ, Roberts NM, Fowler HJ, Roberts MJ, Chan SC, Senior CA (2014) Heavier summer downpours with climate change revealed by weather forecast resolution model. Nat Climate Change 4(7):570–576. https://doi.org/10.1038/NCLIMATE2258
Kiehl J, Hack J, Bonan G, Boville B, Briegleb B, Williamson D, Rasch P (1996) Description of the NCAR community climate model (CCM3). NCAR Technical Note NCAR/TN–420+STR, Natl. Cent. for Atmos. Res., Boulder, CO 80307 USA
Leung LR, Ghan SJ (1995) A subgrid parameterization of orographic precipitation. Theor Appl Climatol 52(1):95–118. https://doi.org/10.1007/BF00865510
Mölg T, Kaser G (2011) A new approach to resolving climate-cryosphere relations: Downscaling climate dynamics to glacier-scale mass and energy balance without statistical scale linking. J Geophys Res Atmos. https://doi.org/10.1029/2011JD015669. https://agupubs.onlinelibrary.wiley.com/doi/abs/10.1029/2011JD015669
Nadeem I, Formayer H (2015) Sensitivity studies of high-resolution RegCM3 simulations of precipitation over the European Alps: the effect of lateral boundary conditions and domain size. Theor Appl Climatol. https://doi.org/10.1007/s00704-015-1586-8

Pal J, Small E, Eltahir E (2000) Simulation of regional-scale water and energy budgets: Representation of subgrid cloud and precipitation processes within RegCM. J Geophys Res Atmos 105(D24):29579–29594. https://doi.org/10.1029/2000JD900415

Pal JS, Giorgi F, Bi X, Elguindi N, Solmon F, Gao X, Rauscher SA, Francisco R, Zakey A, Winter J, Ashfaq M, Syed FS, Bell JL, Diffenbaugh NS, Karmacharya J, Konare A, Martinez D, da Rocha RP, Sloan LC, Steiner AL (2007) Regional climate modeling for the developing world: the ICTP RegCM3 and RegCNET. Bull Am Meteorol Soc 88(9):1395. https://doi.org/10.1175/BAMS-88-9-1395

Pavlik D, Söhl D, Pluntke T, Mykhnovych A, Bernhofer C (2012) Dynamic downscaling of global climate projections for Eastern Europe with a horizontal resolution of 7 km. Environ Earth Sci 65(5):1475–1482. https://doi.org/10.1007/s12665-011-1081-1

Prein AF, Langhans W, Fosser G, Ferrone A, Ban N, Goergen K, Keller M, Tölle M, Gutjahr O, Feser F, Brisson E, Kollet S, Schmidli J, van Lipzig NPM, Leung R (2015) A review on regional convection-permitting climate modeling: Demonstrations, prospects, and challenges. Rev Geophys 53(2):323–361. https://doi.org/10.1002/2014RG000475

Rasmussen R, Liu C, Ikeda K, Gochis D, Yates D, Chen F, Tewari M, Barlage M, Dudhia J, Yu W, Miller K, Arsenault K, Grubisic V, Thompson G, Gutmann E (2011) High-resolution coupled climate runoff simulations of seasonal snowfall over colorado: a process study of current and warmer climate. J Climate 24(12):3015–3048. https://doi.org/10.1175/2010JCLI3985.1

Reynolds R, Rayner N, Smith T, Stokes D, Wang W (2002) An improved in situ and satellite SST analysis for climate. J Climate 15(13):1609–1625. https://doi.org/10.1175/1520-0442(2002)015<1609:AIISAS>2.0.CO;2

Schicker I, Seibert P (2009) Simulation of the meteorological conditions during a winter smog episode in the Inn Valley. Meteorol Atmos Phys 103(1):211–222. https://doi.org/10.1007/s00703-008-0346-z

Termonia P, Schaeybroeck BV, Cruz LD, Troch RD, Caluwaerts S, Giot O, Hamdi R, Vannitsem S, Duchêne F, Willems P, Tabari H, Uytven EV, Hosseinzadehtalaei P, Lipzig NV, Wouters H, Broucke SV, van Ypersele JP, Marbaix P, Villanueva-Birriel C, Fettweis X, Wyard C, Scholzen C, Doutreloup S, Ridder KD, Gobin A, Lauwaet D, Stavrakou T, Bauwens M, Müller JF, Luyten P, Ponsar S, den Eynde DV, Pottiaux E (2018) The CORDEX.be initiative as a foundation for climate services in Belgium. Climate Serv 11:49–61. https://doi.org/10.1016/j.cliser.2018.05.001. http://www.sciencedirect.com/science/article/pii/S2405880717300195

Zeng X, Zhao M, Dickinson R (1998) Intercomparison of bulk aerodynamic algorithms for the computation of sea surface fluxes using TOGA COARE and TAO data. J Climate 11(10):2628–2644. https://doi.org/10.1175/1520-0442(1998)011<2628:IOBAAF>2.0.CO;2